Inorg. Chem. **2004**, *43*, 1294–1301

New Lanthanide Complexes for Sensitized Visible and Near-IR Light Emission: Synthesis, ^{1}H NMR, and X-ray Structural Investigation and Photophysical Properties

Silvio Quici,*,† Giovanni Marzanni,‡ Alessandra Forni,† Gianluca Accorsi,§ and Francesco Barigelletti*,§

CNR—Istituto di Scienze e Tecnologie Molecolari, Via Golgi 19, I-20133 Milano, Italy, Dipartimento di Chimica Organica e Industriale dell'Università, Via Golgi 19, I-20133 Milano, Italy, and CNR—Istituto di Sintesi Organica e Fotoreattività, Via P. Gobetti 101, I-40129 Bologna, Italy

Received October 2, 2003

We describe the syntheses, the ^{1}H NMR studies in CD_3OD and D_2O as solvent, the X-ray characterization, and the luminescence properties in D_2O solution of the two complexes **Eu·1** and **Er·1**, where **1** is a dipartite ligand that includes (i) a 1,4,7,10-tetraazacyclododecane-1,4,7-triacetic acid (**DO3A**) unit serving as hosting site for the metal center; and (ii) a phenanthroline unit which plays the role of light antenna for the sensitization process of the metal centered luminescence. In a previous report (*Inorg. Chem.* **2002**, *41*, 2777), we have shown that for **Eu·1** there are no water molecules within the first coordination sphere. X-ray and ^{1}H NMR results reported here are consistent with full saturation of the nine coordination sites within the **Eu·1** and **Er·1** complexes. In addition, these studies provide important details regarding the conformations, square antiprism (SAP) and twisted square antiprism (TSAP), adopted in solution by these complexes. The luminescence results are consistent with both an effective intersystem crossing (ISC) at the light absorbing phenanthroline unit ($\lambda_{exc} = 278$ nm) and an effective energy transfer (en) process from the phenanthroline donor to the cation acceptor (with unit or close to unit efficiency for both steps). In D_2O solvent, the overall sensitization efficiency, ϕ_{se}, is 0.3 and 5×10^{-6}, for **Eu·1** (main luminescence peaks at 585, 612, 699 nm) and **Er·1** (luminescence peak at 1530 nm), respectively. The photophysical properties of both complexes are discussed with reference to their structural features as elucidated by the obtained ^{1}H NMR and X-ray results.

1. Introduction

Luminescent and stable complexes of lanthanide ions are of great interest because of their technological importance, among others, as diagnostic tools,[1] sensors,[2,3] optical fiber lasers and amplifiers,[4] electroluminescent materials,[5] and magnetic molecular materials.[6] The emission properties of this family of complexes are notable and cover an exceptionally wide spectral range: near-infrared (Nd^{3+}, Er^{3+}), red (Eu^{3+}, Pr^{3+}, Sm^{3+}), green (Er^{3+}, Tb^{3+}), and blue (Tm^{3+}, Ce^{3+}).[7] Unfortunately the lanthanide cations are characterized by very low absorption coefficients ($\epsilon \leq 1\ M^{-1}\ cm^{-1}$), which makes it impossible to effectively populate the emitting levels by direct excitation. Furthermore, coordination of solvent molecules to the lanthanide ions causes dramatic effects on their excited levels. For instance, for the most popular solvent, water, enhanced nonradiative deactivation of these levels takes place mostly through vibronic coupling involving the OH oscillators. According to a largely followed strategy, some of these difficulties can be overcome by coordination of the lanthanide ion with ligands bearing suitable chromophores. In this way, light absorption at the ligand units results in the formation of ligand-centered excited states and the emitting levels of the cation are populated by subsequent

* Authors to whom correspondence should be addressed. E-mail: silvio.quici@istm.cnr.it (S.Q.); franz@isof.cnr.it (F.B.).
† CNR—ISTM.
‡ Dipartimento di Chimica Organica e Industriale dell'Università.
§ CNR—ISOF.

(1) Sammes, P. G.; Yahioglu, G. *Nat. Prod. Rep.* **1996**, 1.
(2) Parker, D. *Coord. Chem. Rev.* **2000**, *205*, 109.
(3) Lowe, M. P.; Parker, D. *Inorg. Chim. Acta* **2001**, *317*, 163.
(4) Kuriki, K.; Koike, Y. *Chem. Rev.* **2002**, *102*, 2347.
(5) Kido, J.; Okamoto, Y. *Chem. Rev.* **2002**, *102*, 2357.
(6) Benelli, C.; Gatteschi, D. *Chem. Rev.* **2002**, *102*, 2369.
(7) Maas, H.; Currao, A.; Calzaferri, G. *Angew. Chem., Int. Ed.* **2002**, *41*, 2495.

10.1021/ic035143b CCC: $27.50
Published on Web 01/29/2004

energy transfer (antenna effect). Of course, the ligand system should also feature 8 to 9 binding sites so as to complete the first coordination sphere of the metal ion, thus excluding coordination of solvent molecules.

A great variety of systems have been designed and studied as chelating agents; among others, polyaminopolycarboxylates,[8,9] cryptands,[10] calixarenes,[11,12] podands,[13] and helicates[14,15] have proved to be very useful. Recently, we have reported a new and structurally very simple ligand system, **1**, that includes a 1,4,7,10-tetraazacyclododecane-1,4,7-

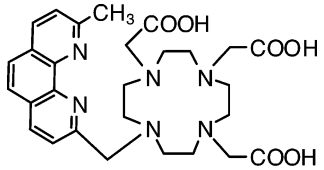

1

triacetic acid (**DO3A**) unit and a phenanthroline unit. The latter serves as a chromophore and is covalently linked to a nitrogen atom of the macrocycle through a methylene spacer. Results obtained with europium(III) and terbium(III) complexes of this ligand showed high overall emission sensitization yields, $\phi_{se} = 0.21$ and 0.11, respectively, in air-equilibrated aqueous solution.[16] Interestingly, our findings based on luminescence results obtained in water and deuterated water indicated that no water molecules are present within the first coordination sphere of the complexes. These results compare well with previous findings from systems to be employed as probes for DNA,[17] where the tetraazacyclododecane unit and the bidentate tetraazatriphenylene ligand[18] were integrated into the complex structure so as to prevent the coordination of water molecules.[19] In these cases, upon excitation at 340 nm, the nine-coordinate complexes of europium(III) and terbium(III) dissolved in water featured emission yields of 0.21 and 0.36, respectively.

Here we report on the syntheses of **Eu·1** and **Er·1** complexes and on the results of studies on their X-ray structure; results on the dynamic behavior of these complexes in CD_3OD and D_2O solution have likewise been obtained. Finally, luminescence results and photophysical properties of the **Eu·1** and **Er·1** complexes in D_2O solution are reported and discussed.

2. Experimental Section

2.1. General. Solvents were purified by using standard methods and dried when necessary. Commercially available reagents were used as received. ^{1}H NMR (300 MHz) spectra were recorded with a Bruker AC 300 and AMX 300 spectrometers. EXSY[20] spectra were collected with 1024 in F_2 and 512 data points in F_1 respectively by using the standard $90°-t_1-90°-t_M-90°$ (NOESY) pulse sequence and the data processed as normally in the COSY experiments.

2.2. Eu·1 Complex. The synthesis and characterization of ligand **1** have been described previously.[16] The complexes were synthesized according to a route outlined in the following for **Eu·1**. A solution of $EuCl_3 \cdot 6H_2O$ (37 mg, 0.1 mmol) in 3 mL of H_2O was slowly added into a magnetically stirred aqueous solution (20 mL) containing ligand **1** (50 mg, 0.09 mmol) and with the pH being kept at 6.5−7.0 by contemporary addition of 5% aqueous NaOH. The solution was then heated at reflux for 4 h, cooled to room temperature, and concentrated to 2 mL by evaporation of the solvent under reduced pressure. The product was purified by column chromatography with Amberlite XAD 1600 eluting first with H_2O, to remove all the inorganic salts, and then with H_2O/CH_3CN 9/1; the pure complex (57 mg, 90%) was recovered as a white solid. Elemental analysis calcd for $C_{28}H_{33}N_6O_6Eu$: C, 47.93; H, 4.75; N, 11.97. Found: C, 47.74; H, 5.10; N, 12.70. MS-FAB+: $m/z =$ 703 [M + H$^+$]; calcd for $C_{28}H_{33}N_6O_6Eu$ $m/z = 702$. For the ^{1}H NMR see Results and Discussion section.

2.3. Er·1 Complex. This compound was isolated in 85% yield as a white solid. Elemental analysis calcd for $C_{28}H_{33}N_6O_6Er \cdot 2H_2O$: C, 44.66; H, 4.96; N, 11.16. Found: C, 44.95; H, 5.21; N, 10.99. MS-FAB+: $m/z = 718$ [M + H$^+$]; calcd for $C_{28}H_{33}N_6O_6Er$ $m/z = 717$. For the ^{1}H NMR see Results and Discussion section.

2.4. Crystallography. A summary of the experimental details is reported in Table 1. The crystals of **Eu·1** and **Er·1** used for the data collections were glued onto a glass fiber with perfluorinated oil and slowly cooled to 150 K in a Kryoflex Bruker cooling device (N_2 gas stream). X-ray data were collected on a Bruker Smart Apex CCD area detector, and data reduction was made using SAINT programs; absorption corrections based on multiscan were obtained by SADABS.[21] The structures were solved by SIR92[22] and refined on F^2 by full-matrix least-squares using SHELX97.[23] For molecular graphics the program ORTEP-III[24] was used. The hydrogen atoms of the complexes were included as riding in calculated positions. The Fourier difference map allowed the location of the oxygen atoms of seven crystallization water molecules. In both structures they were disordered and their position was only partially rationalized. Water hydrogens were not located.

2.5. Photophysical Measurements. Absorption spectra were measured at room temperature in 10^{-5} M water solutions with a

(8) Latva, M.; Takalo, H.; Mukkala, V.-M.; Matachescu, C.; Rodriguez-Ubis, J. C.; Kankare, J. *J. Lumin.* **1997**, *75*, 149.
(9) Takalo, H.; Mukkala, V.-M.; Meriö, L.; Rodriguez-Ubis, J. C.; Sedano, R.; Juanes, O.; Brunet, E. *Helv. Chim. Acta* **1997**, *80*, 732.
(10) Sabatini, N.; Guardigli, M.; Lehn, J.-M. *Coord. Chem. Rev.* **1993**, *123*, 201.
(11) Sabatini, N.; Guardigli, M.; Mecati, A.; Balzani, V.; Ungaro, R.; Ghidini, E.; Casnati, A.; Pochini, A. *J. Chem. Soc., Chem. Commun.* **1990**, 878.
(12) Stemers, F. J.; Verboom, W.; Reinhoudt, D. N.; van der Tol, E. B.; Verhoeven, J. W. *J. Am. Chem. Soc.* **1995,** *117*, 9408.
(13) Armaroli, N.; Accorsi, G.; Barigelletti, F.; Couchman, S. M.; Fleming, J. S.; Harden, N. C.; Jefery, J. C.; Mann, K. L. V.; McCleverty L. J. A.; Rees, H.; Starling, S. R.; Ward, M. D. *Inorg. Chem.* **1999**, *38*, 5769.
(14) Piguet, C. G.; Bünzli, J.-C.; Berardinelli, G.; Bochet, C. G.; Froidevaux, P. *J. Chem. Soc., Dalton Trans.* **1995**, 83.
(15) Lessman, J. J.; Horrocks, W. DeW., Jr. *Inorg. Chem.* **2000**, *39*, 3114.
(16) Quici, S.; Marzanni, G.; Cavazzini, M.; Anelli, P. L.; Botta, M.; Gianolio, E.; Accorsi, G.; Armaroli, N.; Barigelletti, F. *Inorg. Chem.* **2002**, *41*, 2777.
(17) Bobba, G.; Frias, J. C.; Parker, D. *Chem. Commun.* **2002**, 890.
(18) van der Tol, E. B.; van Ramesdonk, H. J., Verhoeven, J. W.; Steemers, F. J.; Kerver, E. G.; Verboom, W.; Reinhoudt, D. N. *Chem. Eur. J.* **1998**, *4*, 2315.
(19) Parker, D.; Dickins, R. S.; Pushmann, H.; Crossland, C.; Howard, J. A. K. *Chem. Rev.* **2002**, *102*, 1977.
(20) Jenkins, B. G.; Lauffer, R. B. *J. Magn. Reson.* **1988**, *80*, 328.
(21) *SMART*, *SAINT*, and *SADABS*; Bruker AXS Inc.: Madison, WI, 1997.
(22) Altomare, A.; Cascarano, G.; Giacovazzo, C.; Guagliardi, A.; Burla, M. C.; Polidori, G.; Camalli, G. *J. Appl. Crystallogr.* **1994**, *27*, 435.
(23) Sheldrick, G. M. *SHELX-97. Program for the Refinement of Crystal Structures*; University of Göttingen: Göttingen, Germany, 1997.
(24) Burnett, M. N.; Johnson, C. K. *ORTEP-III: Oak Ridge Thermal Ellipsoid Plot Program for Crystal Structure Illustrations*; Oak Ridge National Laboratory Report ORNL-6895; Oak Ridge National Laboratory: Oak Ridge, TN, 1996.

Table 1. Crystal Data, Details of Data Collection, and Results of the Refinement for **Eu·1** and **Er·1**

	Eu·1	Er·1
formula	$Eu(C_{28}H_{33}N_6O_6)\cdot 7H_2O$	$Er(C_{28}H_{33}N_6O_6)\cdot 7H_2O$
M_r	813.56	828.86
space group	triclinic $P\bar{1}$	triclinic $P\bar{1}$
Z	2	2
D_{calc} (g cm^{-3})	1.600	1.656
a (Å)	11.033(2)	10.960(2)
b (Å)	11.219(2)	11.224(2)
c (Å)	16.082(3)	15.926(3)
α (deg)	83.98(1)	83.02(1)
β (deg)	73.14(1)	73.07(1)
γ (deg)	62.46(1)	62.53(1)
V (Å^3)	1688.2(5)	1662.6(6)
cryst dimens (mm)	0.32 × 0.22 × 0.12	0.20 × 0.08 × 0.04
color, habit	colorless, prism	colorless, prism
μ (mm^{-1})	1.929	2.596
radiation	Mo Kα	Mo Kα
T (K)	150(2)	150(2)
$2\theta_{max}$ (deg)	65.74	65.96
h, k, l ranges	−16 → 16; −17 → 17; −24 → 24	−16 → 16; −17 → 16; −24 → 24
intensity decay	none	none
adsorption correction	multiscan (Bruker SADABS)	multiscan (Bruker SADABS)
T_{min}, T_{max}	0.849, 1.000	0.862, 1.000
measd reflns	29815	26265
R_{int}	0.022	0.0398
indep reflns	11510	11341
reflections with $I > 2\sigma(I)$	10682	9144
no. of parameters	605	488
$R(F^2)$, $wR(F^2)$	0.0303, 0.0817	0.0561, 0.1174
$R[F^2 > 2\sigma(F^2)]$, $wR[F^2 > 2\sigma(F^2)]$	0.0273, 0.0737	0.0389, 0.0888
goodness-of-fit	1.109	1.035
$(\Delta/\sigma)_{max}$	0.006	0.001
$\Delta\rho_{max}$, $\Delta\rho_{min}$ (e Å^{-3})	1.521, −0.823	1.418, −1.464

Perkin-Elmer Lambda 5 UV/vis spectrophotometer; the absorption profiles for the complexes correspond to that for the phenanthroline chromophore, as previously determined for **Eu·1**.[16] On this basis, for the steady-state luminescence experiments performed at room temperature, in air-equilibrated or argon-bubbled samples, the selected excitation wavelength was 278 nm. The luminescence spectra were registered either with a Spex Fluorolog II spectrofluorimeter equipped with Hamamatsu R928 phototube or with an Edinburgh FLS920 spectrometer equipped with Hamamatsu R5509-72 supercooled photomultiplier tube (193 K), and a TM300 emission monochromator with NIR grating blazed at 1000 nm; 150 and 450 W xenon arc lamps were used, respectively, as light sources. Corrected luminescence spectra in the range 500−820 nm were then obtained by taking care of the wavelength dependence of the phototube response. Relative luminescence intensities were evaluated from the area (on an energy scale) of the luminescence spectra and with reference to a luminescence standard $[Ru(bpy)_3]Cl_2$ ($\phi = 0.028$ in air-equilibrated water).[16,25]

For the visible region, luminescence lifetimes on the millisecond time scale were obtained with a Perkin-Elmer LS50B luminescence spectrometer. The experimental uncertainty on the absorption and luminescence maxima is 2 and 1 nm, respectively; that for the ϕ and τ values is 10%.

3. Results and Discussion

3.1. Structural Investigation by ^{1}H NMR Spectroscopy. Nowadays NMR spectroscopy has been largely applied for the study of structure and dynamic behavior of molecules in solution mostly because of the development of new technologies and of more sophisticated techniques of investigation. In the case of metal complexes, NMR spectroscopy can give an indication about the geometry of the coordinated binding sites around the metal cation and of the stability of the resulting complexes.

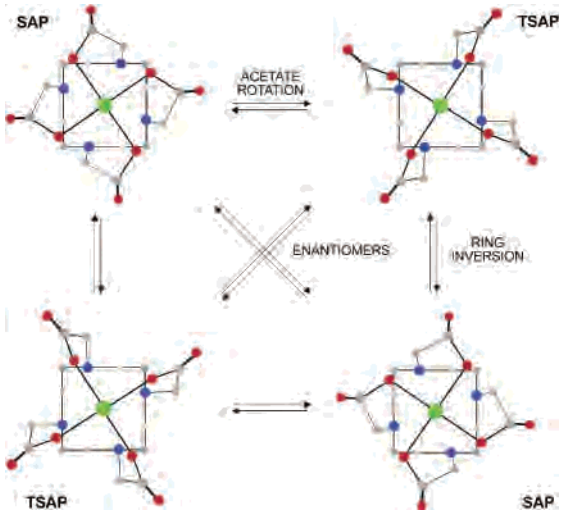

Figure 1. Possible isomers of lanthanide−DOTA complexes.

The ^{1}H NMR analysis of lanthanide metal complexes is complicated by the high paramagnetic character of these metal ions and by the possible conformational equilibria that are present in solution when polyaminepolycarboxylic ligands are involved. It is known from the literature that lanthanide complexes with 1,4,7,10-tetraazacyclododecane-1,4,7,10-tetraacetic acid (**DOTA**) are present in two possible isomeric conformations, square antiprism (SAP) and twisted square antiprism (TSAP), and these can interconvert either by ring inversion or by rotation of the acetate arms (Figure 1).[26]

It is evident that a single process results in a change in the geometry of the complex from SAP to TSAP, and vice versa, while both processes in a concerted manner result in the exchange of enantiomeric pairs with retention of the geometry. By considering the relationship between the rate of the interconversion process and the NMR time scales three limit situations can be encountered: (i) Fast exchange, when the interconversion rate is faster with respect to the NMR time scale. In this case, an averaged situation is detected and the signal is positioned at a frequency which is a weighted average of the molar fraction of the frequencies of the exchanging signals. (ii) Moderately slow exchange. In this case, a significant broadening of the signals is observed. (iii) Slow exchange, when the interconversion process is slow with respect to the NMR time scale. In this case it is possible to observe a distinct set of signals for each conformation present in solution.

The high resolution ^{1}H NMR spectrum of **Yb·1** in D_2O solution evidenced only the square antiprism isomer in a range of temperature from 0 °C to 80 °C,[16] which is

(25) Nakamaru, K. *Bull. Chem. Soc. Jpn.* **1982**, *55*, 2967.
(26) Marques, M. P. M.; Geraldes, C. F. G. C.; Sherry, A. D.; Merbach, A. E.; Powell, H.; Pubanz, D.; Aime, S.; Botta, M. *J. Alloys Compound* **1995**, *225*, 303.

consistent with literature data reported for **Yb·DOTA** which indicate SAP as the predominant isomer.[27] This result suggests that at least one nitrogen atom of phenanthroline (that adjacent to the methylene group) in the **Yb·1** complex coordinates the metal ion giving a five membered ring particularly stable in the case of lanthanide complexes.[28] Furthermore, the absence of water molecules directly coordinated to the metal ion in the **Eu·1** complex[16] can be considered as a clear indication that also the second nitrogen atom is involved in the first coordination sphere thus giving a nine coordinated Yb^{3+}. Unfortunately, the NMR data alone did not allow a firm conclusion about having a nine-coordinated or eight-coordinated complex. In this last case the access of water molecules on the first coordination sphere of the metal could perhaps be prevented because of the steric hindrance of the rigid phenanthroline group.[16]

Therefore, we performed a more detailed ^{1}H NMR investigation aimed to get more information on the coordination geometry and conformational equilibria of **Eu·1** and **Er·1** in CD_3OD and D_2O solution, respectively.

The ^{1}H NMR spectrum of a 0.038 M solution of **Eu·1** in CD_3OD at room temperature shows very broad resonances and covers a large spectral width (from +75 to − 25 ppm). By lowering the temperature, the resonances spread over a large chemical shift range, from 80 to −45 ppm, and a progressive resolution of the spectrum is observed (Figure 2a). The resolution is complete at 223 K (Figure 2b).

At this temperature two sets of signals are observed, one of which, composed of 31 distinct signals corresponding to 31 nonequivalent protons, strongly predominates. All the resonances have the same relative intensity with the exception of that at 46.5 ppm, relative intensity 3, which is safely attributed to the CH_3 of the phenanthroline.

By comparing the ^{1}H NMR spectrum of **Eu·1** with that of **Yb·1** and according to literature results,[26,29,30] we can conclude that the predominant species in solution is the isomer with square antiprism geometry together with a small amount of the isomer having twisted square antiprism geometry. These results indicate that the exchange rate is moderately slow at room temperature while at 233 K it becomes sufficiently slow making it possible to observe both the SAP and TSAP isomers. Accordingly the EXSY spectrum at 233 K clearly shows the exchange between each signal of the major isomer with the corresponding signal of the minor isomer. In Figure 3b the exchange of the signals in the 80−15 ppm spectral region between the two isomers is highlighted as an example.

By comparing the ^{1}H NMR results obtained with **Eu·1** and **Yb·1** complexes we can conclude that in the former case the Eu^{3+} (which is in the middle of the lanthanide series) can stabilize both the SAP and TSAP isomers while the Yb^{3+} (which is at the end of the series) stabilizes preferentially the SAP geometry.[31]

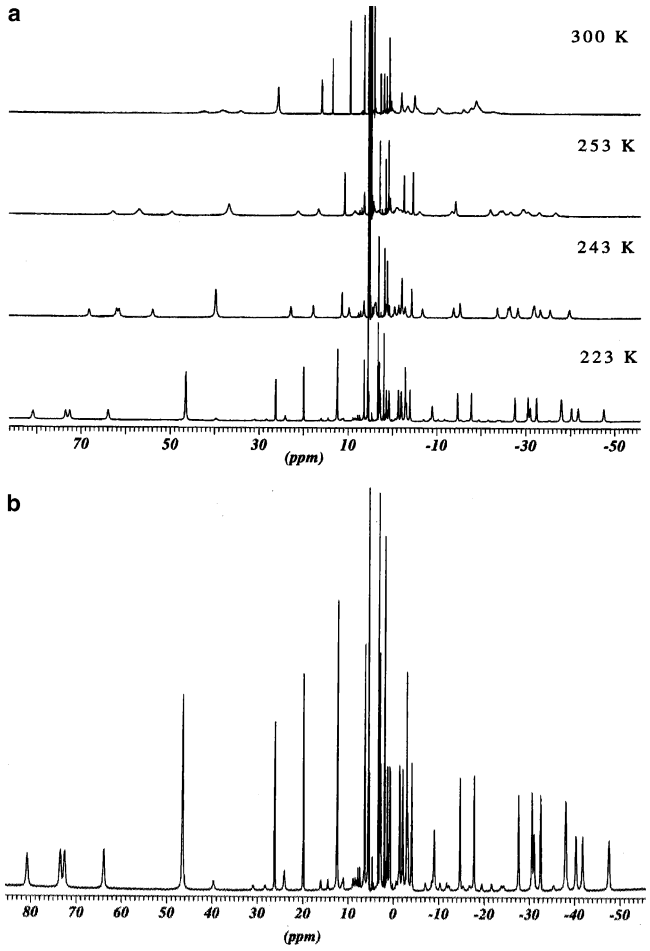

Figure 2. (a) 300 MHz variable temperature ^{1}H NMR spectra of **Eu·1** in CD_3OD. (b) ^{1}H NMR spectrum of **Eu·1** in CD_3OD at 223 K.

The ^{1}H NMR analysis of **Er·**1 proved to be more complicated probably because of the electronic properties of the metal. The spectrum is completely resolved at 295 K and covers a spectral width of 450 ppm. Again it is possible to identify 31 nonequivalent signals which are broader than usual, indicating very small t_2 values, which makes it impossible to perform a bidimensional ^{1}H NMR analysis. Indeed the transfer of magnetization is destroyed by fast relaxation processes. Variable temperature ^{1}H NMR experiments registered in D_2O indicate the presence of coalescence processes, and the limit situation is observed at 363 K (Figure 4).

By comparison with **Yb·1** and **Eu·1** we can conclude that in the case of **Er·1** complex only the SAP isomer is present.

3.2. Structural Investigation by X-ray Analysis. Crystal data and the results of the least-squares refinement for complexes **Eu·1** and **Er·1** are reported in Table 1, while in Figure 5 the structure of the Eu complex is shown. The **Eu·1·**$7H_2O$ and **Er·1·**$7H_2O$ complexes are isomorphous.

The metal ion is in a nine-coordinate ligand environment comprising the four nitrogens of the tetraazacyclododecane ring, the three carboxylate oxygens, and the two phenanthroline nitrogen atoms. No water molecules are involved in the metal coordination sphere. The coordination geometry

(27) Aime, S.; Botta, M.; Ermondi, G. *Inorg. Chem.* **1992,** *31,* 4291.
(28) Aime, S.; Batsanov, A. S.; Botta, M.; Howard, J. A. K.; Lowe, M. P.; Parker, D. *New J. Chem.* **1999**, *23*, 669.
(29) Desreux, J. F. *Inorg. Chem.* **1980**, *19*, 1319.
(30) Benetollo, F.; Bombieri, G.; Calabi, L.; Aime, S.; Botta, M. *Inorg. Chem.* **2003**, *42*, 148.
(31) Bunzly, J. C. G.; Piguet, C. *Chem. Rev.* **2002**, 102, 1897.

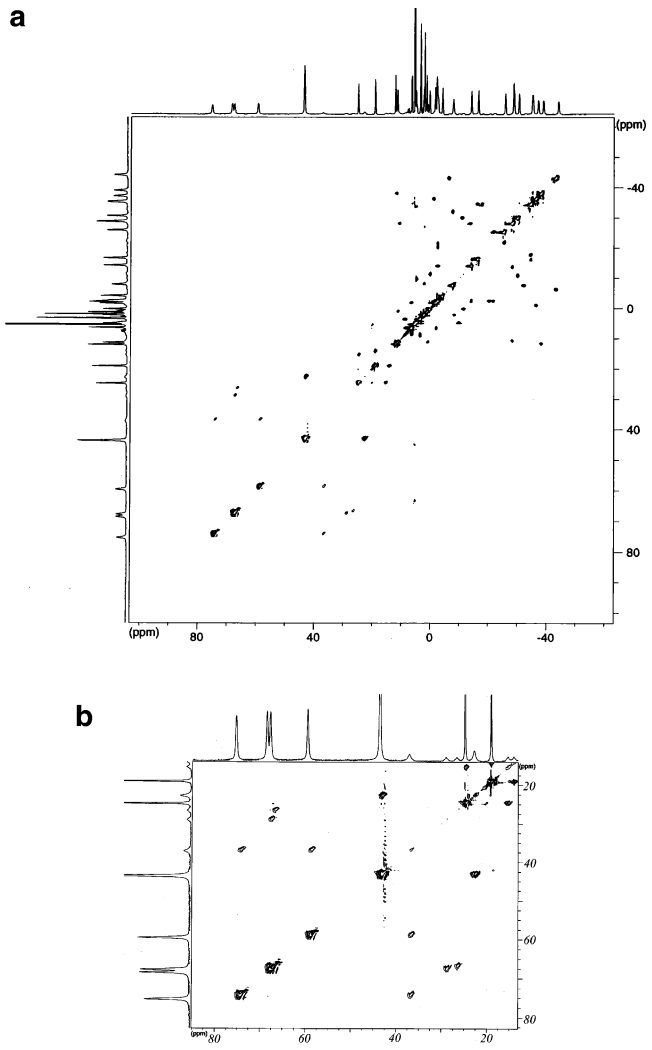

Figure 3. (a) EXSY spectrum of **Eu·1** at 233 K. (b) EXSY spectrum of **Eu·1** at 233 K highlighted in the 20−80 ppm chemical shift range.

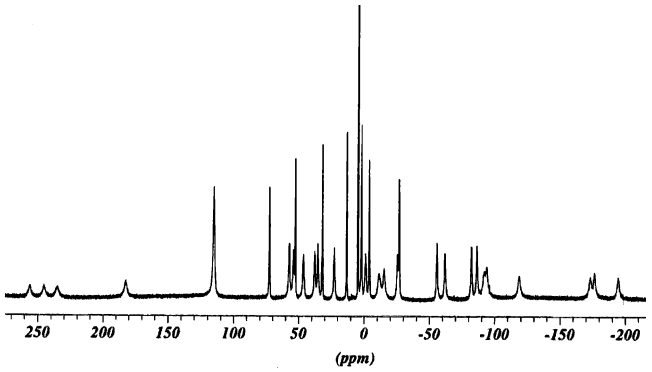

Figure 4. 300 MHz ^{1}H NMR spectrum of **Er·1** in D_2O at 363 K.

is capped square antiprismatic, with the four ring nitrogens on one basal plane, the three carboxylate oxygens and the N5 phenanthroline nitrogen on the other basal plane, and the N6 phenanthroline nitrogen capping the latter.

In crystals of the **Eu·1** complex the tetraazacyclododecane ring assumes in the crystal two alternative and equiprobable conformations, labeled with **A** and **B** (in Figure 5 only the **A** conformation is shown). In both cases the ring adopts the usual quadrangular [3333] conformation,[32] with ag^+g^+ units

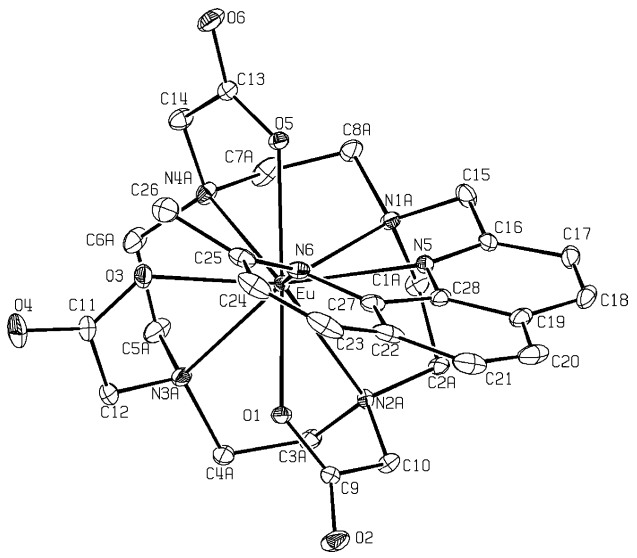

Figure 5. Molecular structure of [**Eu·1**]·7H_2O with hydrogens omitted for clarity. The water molecules are not shown. Displacement ellipsoids are drawn at the 20% probability level. The same atom numbering scheme was adopted for the [**Er·1**]·7H_2O complex.

on going along the ring from N1 toward N2 and so on in the case of **A**, and ag^-g^- units moving in the opposite direction from N1 toward N4 for **B**. The corresponding torsion angles are on the average −163.9(3)°, 60.4(4)°, 77.0(4)° and 162.8(3)°, −58.1(4)°, −79.7(4)° for **A** and **B**, respectively. The four nitrogen atoms of the ring are coplanar within the experimental error for both the conformations. The atoms of the other basal plane, O_3N, undergo a slight tetrahedral distortion, with O1 and O5 on the side of the Eu^{3+} ion, at 0.025(2) and 0.029(2) Å, respectively, from the least-squares plane of the four basal atoms, and O3 and N5 on the other side, at 0.033(2) and 0.034(2) Å, respectively, from the same plane. The two N_4 and O_3N planes are parallel within 4.1(1)°, when considering the tetraazacyclododecane ring in the **A** conformation, and within 3.3(1)° in the case of the **B** conformation. The Eu^{3+} ion is placed at 1.6605(2)/1.7467(2) and 0.7718(2) Å from the N_4 (**A**/**B** conformation) and the O_3N planes, respectively. The two basal planes are twisted by 9/23° with respect to the ideal twisting angle of the square antiprism geometry. By comparison of these results with the twist angles reported in the literature, conformations **A** and **B** can be safely assigned to SAP and TSAP geometry, respectively.

For the case of **Er·1** the tetraazacyclododecane ring assumes in the crystal only the conformation with ag^+g^+ units moving from N1 toward N2, the corresponding torsion angles measuring, on the average, −164.3(2)°, 59.4(3)°, and 78.3(3)°, respectively. The four nitrogen atoms of the ring are strictly coplanar, while the atoms of the O_3N basal plane are subjected to a similar but slightly larger distortion with respect to complex **Eu·1**. The four atoms deviate from their least-squares plane by 0.032(3) and 0.034(3) Å (atoms O1 and O5), and by 0.039(3) and 0.048(3) Å (atoms O3 and N5). The two basal planes are parallel within 3.46(8)° and twisted by 8° with respect to the ideal twisting angle of the

(32) Dale, J. *Isr. J. Chem.* **1980**, *20*, 3.

Table 2. Selected Bond Lengths (Å) and Angles (deg) for **Eu·1**·7H_2O and **Er·1**·7H_2O

	Eu·1·7H_2O	**Er·1**·7H_2O
M−O1	2.343(2)	2.287(3)
M−O3	2.331(2)	2.269(3)
M−O5	2.353(2)	2.289(3)
M−N1	2.702(6), 2.742(5)[a]	2.634(4)
M−N2	2.682(5), 2.770(6)[a]	2.675(3)
M−N3	2.667(11), 2.718(10)[a]	2.628(4)
M−N4	2.682(9), 2.612(10)[a]	2.612(3)
M−N5	2.522(2)	2.439(3)
M−N6	2.773(2)	2.728(3)
O1−M−O3	86.16(7)	86.10(11)
O1−M−O5	142.98(7)	143.06(10)
O1−M−N5	87.02(7)	86.05(11)
O1−M−N6	69.24(7)	68.78(10)
O3−M−O5	82.86(7)	83.50(11)
O3−M−N5	140.73(8)	139.92(11)
O3−M−N6	80.22(7)	78.50(11)
O5−M−N5	79.71(7)	79.62(11)
O5−M−N6	74.09(6)	74.43(10)
N5−M−N6	61.26(7)	62.04(11)
N1−M−N2	65.6(2), 63.0(2)	65.61(11)
N1−M−N3	103.3(3), 99.8(3)[a]	103.80(12)
N1−M−N4	67.7(2), 67.8(2)[a]	68.99(11)
N2−M−N3	68.0(2), 64.4(2)[a]	67.52(11)
N2−M−N4	103.7(2), 99.2(2)[a]	104.32(11)
N3−M−N4	68.4(2), 66.2(3)[a]	68.97(11)

[a] First and second values refer to the **A** and **B** conformations of the tetraazacyclododecane ring, respectively.

square antiprism geometry. The Er^{3+} ion is placed at 1.6211(2) and 0.7564(2) Å from the N_4 and the O_3N planes, respectively.

Selected geometric parameters for the two complexes are reported in Table 2. A comparison between corresponding bond lengths in the two complexes indicates a systematic and significant contraction on going from **Eu·1** to **Er·1** according to the lower atomic radius of Er^{3+} with respect to Eu^{3+} ion. The contraction amounts to 0.060 Å for both the Ln−O and the Ln−N average distances involving the nitrogen atoms of the tetraazacyclododecane ring. The Ln−N5 and Ln−N6 bond lengths decrease by 0.083 and 0.045 Å, respectively. In both complexes, all the Ln−N distances are much longer than the average Ln−O distance (2.342 and 2.282 Å in **Eu·1** and **Er·1**, respectively), according to what is generally observed in polyaminopolycarboxylate complexes. In particular, for the 16 structures of Eu complexes with **DOTA** derivatives, as retrieved from a survey on the Cambridge Structural Database (CSD version 5.24, no refcode restrictions applied),[33] the Eu−N and Eu−O average distances are 2.671 and 2.395 Å, respectively. When considering the set of the lanthanide ion−nitrogen (Ln−N) bond lengths in **Eu·1** and **Er·1**, significant differences are to be noticed. The distances between the Ln ion and the phenanthroline nitrogen N5 taking part to the O_3N basal plane, 2.522 Å in **Eu·1** and 2.439 Å in **Er·1**, are much shorter than the average Ln−N distances involving the nitrogen atoms of the tetraazacyclododecane ring (2.697 Å in Eu·**1** and 2.637 Å in Er·**1**). On the other hand, the distances of the N6 phenanthroline nitrogen atom from the Ln ion, 2.773 Å in **Eu·1** and 2.728 Å in **Er·1**, are the larger ones between the whole set of Ln−N distances.

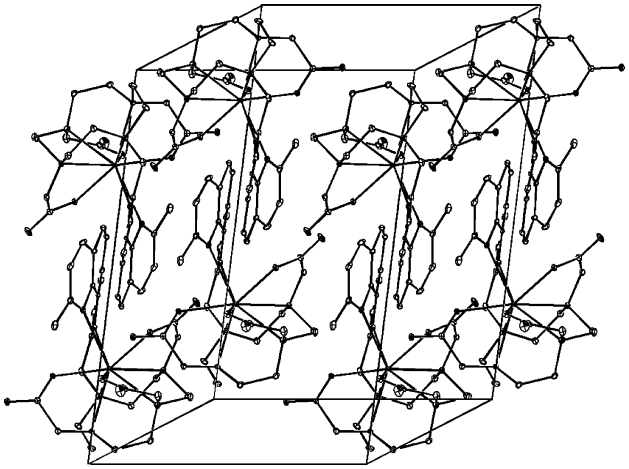

Figure 6. Crystal packing view along *a* of [**Er·1**]·7H_2O. Hydrogen atoms and water molecules are omitted for clarity.

Unexpectedly, the phenanthroline moiety in both complexes undergoes a remarkable distortion with respect to the uncoordinated molecule.[34] The three rings taken separately deviate significantly from planarity, and, on the whole, they are characterized by a large curvature as imposed by the present double coordination to the metal ion through the N5 and N6 atoms. By considering the least-squares plane of the central ring, the greater deviations are observed for the atoms C24 and C25, from one side of the ring, and for the atom C17, from the other side. They are placed at 0.570(4), 0.495(3), and 0.395(3) Å from this plane, respectively, in **Eu·1** and at 0.583(6), 0.499(5), and 0.450(5) Å, respectively, in **Er·1**.

The crystal packing of the Er complex is reported in Figure 6.

In both crystal structures the complex molecules are linked by chains of noncoordinated water molecules. Moreover, the phenanthroline moieties of molecules connected by the $-x, -y, -z + 1$ and $-x - 1, -y, -z + 1$ symmetry operations are parallel to one another allowing $\pi-\pi$ stacking interactions between them. The shortest contacts between phen units connected by these operations are 3.267(7), 3.228(10) Å ($C23\cdots C24_{-x,-y,-z+1}$), and 3.442(5), 3.456(7) Å ($N6\cdots C17_{-x-1,-y,-z+1}$), in **Eu·1** and **Er·1**, respectively. Such interactions, together with hydrogen bonding, lead to the stabilization of the crystal.

3.3. Luminescence and Photophysical Properties. The antenna-to-cation sensitization process includes a sequence of steps, see Figure 7.

These are (i) light absorption at the phenanthroline chromophore to produce the singlet (S) excited state, (ii) intersystem crossing (ISC) to populate the lowest-lying triplet (T) level, (iii) energy transfer from this level to the available manifold of metal-centered (MC) excited levels, (iv) population of the MC luminescent level and light emission. Accordingly, the overall efficiency for the sensitized emission, ϕ_{se}, is[16,35,36]

$$\phi_{se} = \phi_{ISC}\phi_{en}\phi_{lum}^{MC}$$

(33) Allen, F. H. *Acta Crystallogr., Sect. B* **2002**, *58*, 380.

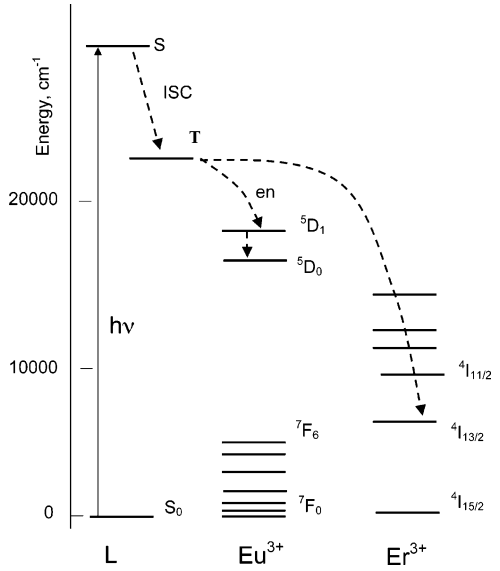

Figure 7. Energy levels for complexes **Eu·1** and **Er·1**.

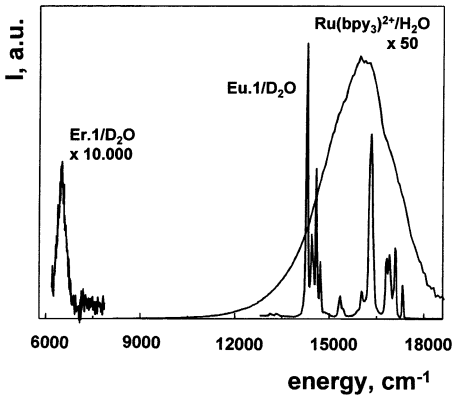

Figure 8. Luminescence spectra for **Eu·1** and **Er·1**, and $[Ru(bpy)_3]^{2+}$ complexes in the indicated solvents; excitation of isoabsorbing samples (absorbance 0.15) was performed at 278 nm.

For the complexes **Eu·1** and **Er·1**, excitation in correspondence of the intense ligand absorption at 278 nm ($\epsilon = 17000\ M^{-1}\ cm^{-1}$) results in sensitization of the metal-centered luminescence, see Figure 8. On the basis of the photophysical properties of the phenanthroline unit, $\phi_{ISC} = 1$ and ligand-to-metal energy transfer is expected to originate from the triplet level of this chromophore, $E_T = 21830\ cm^{-1}$, with lifetime $\tau_T = 35$ ms.[16,37]

For **Eu·1**, the energy gap between the higher-lying T level of the ligand and the $^5D_0$ level of Eu^{3+} is $\Delta E \approx 4500\ cm^{-1}$.[16] It is of relevance that deactivation of the T level by oxygen quenching is not observed, i.e., air-equilibrated and argon-bubbled samples yield the same intensity of the luminescence spectra. Given that the rate constant for competitive quenching by oxygen in water is $k_q^{O_2} = 2.0 \times 10^6\ s^{-1}$,[16] this is consistent with the energy transfer rate constant being $k_{en} \geq 1 \times 10^7\ s^{-1}$. As a consequence, it is concluded that for **Eu·1** the ligand-to-cation energy transfer step favorably competes against both intrinsic phosphorescence decay and oxygen quenching, and $\phi_{en} = 1$. The same line of reasoning applies to the case of **Er·1**, whose luminescent level is ascribed to the $^4I_{13/2} \rightarrow {}^4I_{15/2}$ transition,[38,39] peaking at 1530 nm, so that $\Delta E \approx 15300\ cm^{-1}$. Also for this complex, no oxygen effect is observed and it is concluded that energy transfer is exclusively responsible for deactivation of the ligand T level. In conclusion, for both **Eu·1** and **Er·1**, $\phi_{ISC} \times \phi_{en} = 1$,[40] and the overall sensitizing process is regulated by the metal centered photophysics,

$$\phi_{se} = \phi_{lum}{}^{MC}$$

Table 3. Photophysical Parameters in D_2O

	$\phi_{ISC}\phi_{en}$	ϕ_{MC}	τ_{MC}, s	k_r, s^{-1}	k_{nr}, s^{-1} [a]	q^b
Eu·1	1	0.3	1.77×10^{-3}	170[a]	395[a]	0.0
Er·1	1	5×10^{-6}	$<0.1 \times 10^{-6}$ [c]	125[d]	2.5×10^7 [a]	

[a] According to $k_r = \phi_{MC}/\tau_{MC}$ and $k_{nr} = 1/\tau_{MC} - k_r$. [b] Water molecules of the coordination sphere, $q^{Eu} = 1.2(1/\tau_{MC}{}^{H_2O} - 1/\tau_{MC}{}^{D_2O} - 0.25)$, where the lifetimes are in millliseconds and the measured τ^{H_2O} was 1.24 ms; the uncertainty for q is estimated ± 0.5; see: Beeby, A.; Clarkson, I. M.; Dickins, R. S.; Faulkner, S.; Parker, D.; Royle, L.; de Sousa, A. S.; Williams, J. A. G.; Woods, M. *J. Chem. Soc., Perkin Trans. 2* **1999**, 493 and ref 42. [c] Estimated on the basis of $\tau_{Er} = \phi_{MC}/k_r$. [d] From ref 42.

Table 3 compares photophysical properties for the **Eu·1** and **Er·1** complexes; the solvent employed was D_2O because in H_2O luminescence of Er^{3+} is not observed. It is worth noticing the low luminescence quantum yield for the case of **Er·1**, $\phi_{Er} = 5 \times 10^{-6}$. This value appears one,[41] or two,[39] orders of magnitude lower than what is found in other complexes of Er^{3+}. It should be stressed however that most literature data regarding ϕ_{Er} has been drawn relying on a comparison between observed and radiative lifetimes, according to $\phi_{Er} = \tau_{obs}/\tau_{rad}$.[38,39,42] Our approach has been to proceed to a direct comparison of calculated areas (in cm^{-1}) for the luminescence profiles as obtained from corrected luminescence spectra and by using isoabsorbing solutions at the selected excitation wavelength, 278 nm. A largely employed luminophore, $[Ru(bpy)_3]^{2+}$ ($\phi = 0.028$ in aerated water),[16] has been selected as a standard, because it exhibits both a reasonable spectral overlap (see Figure 8), and an intermediate value of luminescence quantum yield with respect to the cases of **Eu·1** and **Er·1**, see Table 3.

4. Conclusions

The synthesis and structural and functional characterization of Eu^{3+} and Er^{3+} complexes of a dipartite ligand **1** have been described. This ligand contains 1,4,7,10-tetraazacyclododе-

(34) Nishigaki, S.; Yoshioka, H.; Nakatsu, K. *Acta Crystallogr., Sect. B* **1978**, *34*, 875.
(35) Klink, S. I.; Grave, L.; Reinhoudt, D. N.; van Veggel, F.; Werts, M. H. V.; Geurts, F. A. J.; Hofstraat, J. W. *J. Phys. Chem. A* **2000**, *104*, 5457.
(36) Beeby, A.; Faulkner, S.; Parker D.; Williams, J. A. G. *J. Chem. Soc., Perkin Trans. 2* **2001**, 1268.
(37) Murov, S. L.; Carmichael I.; Hug, G. L. *Handbook of Photochemistry*; M. Dekker: New York, 1993.
(38) Werts, M. H. V.; Hofstraat, J. W.; Geurts F. A. J.; Verhoeven, J. W. *Chem. Phys. Lett.* **1997**, *276*, 196.
(39) Werts, M. H. V.; Verhoeven J. W.; Hofstraat, J. W. *J. Chem. Soc., Perkin Trans. 2* **2000**, 433.
(40) In correspondence to the E_T level there is a sufficiently dense manifold of excited levels of Er^{3+},[36] which can therefore play as acceptor levels for energy transfer.
(41) Hebbink, G. A.; Grave, L.; Woldering, L. A.; Reinhoudt D. N.; van Veggel, F. *J. Phys. Chem. A* **2003**, *107*, 2483.
(42) Weber, M. J. *Phys. Rev.* **1968,** *171*, 283.

cane-1,4,7-triacetic acid (**DO3A**) as a recognition site for the lanthanide ions and an asymmetrically substituted phenanthroline moiety covalently linked, through one methylene spacer, to the fourth nitrogen atom of the macrocyclic ring as a chromophore. For **Eu·1** in CD_3OD, the ^1H NMR study evidences the presence of two isomers having square antiprism (SAP) and twisted square antiprism (TSAP) geometry, with the former being predominant, according to literature data for **Eu·DOTA** complex.[30] The ^1H NMR resonances of these isomers are better resolved by lowering the temperature, the optimum being observed at 223 K. The EXSY spectrum of **Eu·1** at this temperature indicates that there is exchange between the resonances of the major isomer with the corresponding resonances of the minor isomer. In the case of **Er·1**, ^1H NMR results in D_2O are consistent with the presence of only the SAP isomer, as observed also for **Yb·1**.[16]

X-ray analysis of **Eu·1** and **Er·1** complexes indicates that in both cases the metal ion is nine-coordinated, with the apical position being occupied by the distal nitrogen atom of the phenanthroline unit. Unexpectedly, the planarity of the phenanthroline is severely distorted because of this coordination. Indeed, the photophysical results confirm that no water molecules are present in the first solvation sphere of the metal. For **Eu·1** and **Er·1** in D_2O, the lanthanide-based luminescence is observed with quantum yields of 0.30 and 5×10^{-6}, respectively. The relatively low values for ϕ_{Er} could be ascribed to the effect of various types of vibrations around the cation, because both **DO3A** and the spatially close phenanthroline unit cooperatively play as hosting site for Er^{3+} center. Interestingly, the results of the structural investigation of **Eu·1** and **Er·1** indicate that substitution of one acetate residue of **DOTA** with a chelating group having the donor sites correctly positioned to coordinate the metal ion (such as in the case of phenanthroline) does not compromise the coordination properties of **1**, with respect to those of **DOTA**, either in solution or in the solid state.

Acknowledgment. Financial support by Fondo Integrativo per la Ricerca di Base (FIRB) of MIUR, Project RBNE019H9K entitled "Nanometric machines through molecular manipulation", is gratefully acknowledged.

Supporting Information Available: X-ray crystallographic file in CIF format for **Eu·1** and **Er·1**. This material is available free of charge via the Internet at http://pubs.acs.org.

IC035143B